ACS Photonics
pubs.acs.org/journal/apchd5
Comment

# Comment on “Upconversion-Assisted Dual-Band Luminescent Solar Concentrator Coupled for High Power Conversion Efficiency Photovoltaic Systems”

Chenchen Yang and Richard R. Lunt*

*ACS Photonics* **2018**, *5* (9), 3621−3627, DOI: 10.1021/acsphotonics.8b00498

Cite This: *ACS Photonics* 2021, 8, 678−681 Read Online





In the recent article by Ha et al., a triplet−triplet annihilation (TTA)-based photon up-conversion (UC) mechanism was combined with a downshifting (DS) process to demonstrate a selective-harvesting semitransparent luminescent solar concentrator (LSC).[1] Both ultraviolet (UV) and red light are absorbed and converted into green light by downshifting and triplet−triplet annihilation up-conversion luminescence,[2−5] respectively, resulting in a reported optimized power conversion efficiency (*PCE*) of 9.1% and an average transmittance of ∼90%.[1] However, the performance metrics of the luminescent solar concentrator−dye-sensitized solar cell (LSC-DSSC) system are clearly overestimated due to poor characterization protocols. In this Comment, we identify the inconsistencies in which the presented data falls short of the reporting for a luminescent solar concentrator−photovoltaic (LSC-PV) system. Many of the points presented here have been outlined in a recent commentary, which describes the best protocols for data collection and necessary consistency checks.[6]

(1) The first key data for reporting a photovoltaic system is the measurement of the current density ($J$)−voltage ($V$) characteristics under standard illumination (AM 1.5G), which are necessary to report the corresponding power conversion efficiency (*PCE*). We emphasize that such data are necessary for all PV and LSC reports, despite many LSC reports missing this data.[6,7] A common mistake in reporting *PCE*s of PVs is the mismeasurement (or incorrect use) of the active device area, which is directly used to calculate the current density from the measured current. Any error in the calculated device area will directly and proportionally propagate to the PCE.[6−8] In LSCs, there are two areas that are typically described (Figure 1A), the area of the waveguide front surface ($A_{LSC}$) and the total area of the waveguide edge ($A_{edge}$).[6,9,10] Once a PV cell (e.g., DSSC, organic PV, perovskite PV, etc.) is edge-mounted onto an LSC waveguide, the LSC-PV system should be treated as an integrated photovoltaic device, and the input solar power is received by the area of the front surface of the LSC waveguide ($A_{LSC}$) rather than the area of the edge-mounted PV ($A_{edge}$). An extreme case is given by comparing LSC-PV systems with various waveguide dimensions in Figure 1A−C: assuming no reabsorption loss within all the LSC-PV systems, the scaling of the generated photocurrent ($I$) is always with respect to the collection area $A_{LSC}$, which is fundamentally tied to the total input solar flux ($I \propto A_{LSC}$), as with other standard PV systems. If $A_{edge}$ is instead applied in the photocurrent density calculation ($J = I/A_{edge}$), the calculated $J$ will approach infinity as the thickness of the waveguide and $A_{edge}$ decrease with constant $A_{LSC}$, easily resulting in *PCE* values above the Shockley−Queisser limit.[11−13] The *PCE* of the LSC-PV system ($\eta_{LSC}$) should always be calculated as follows:

$$\eta_{LSC} = \frac{I_{SC} \cdot V_{OC} \cdot FF}{P_0 \cdot A_{LSC}} = \frac{J_{SC} \cdot V_{OC} \cdot FF}{P_0} \quad (1)$$

where $I_{SC}$ is the short-circuit current acquired from the current−voltage characteristic of the LSC-PV system, $J_{SC}$ is the short-circuit current density obtained from $I_{SC}/A_{LSC}$, $V_{OC}$ is the open-circuit voltage, $FF$ is the fill factor, and $P_0$ is the input power density (e.g., 1000 W/m$^2$). The equivalent approaches for making $J$−$V$ measurements with mounting 1, 2, or 4 cells around the LSC has been described previously.[6]

In the work by Ha et al.,[1] the LSC-DSSC systems were reported based on two waveguide dimensions of 5 cm × 1 cm and 2 cm × 2 cm, as shown in Figures 2C and 4A of the original manuscript,[1] and $J$−$V$ characteristics were used to calculate the PCE of the LSC-DSSC system. However, both the $A_{LSC}$ and $A_{edge}$ were applied to calculate the *PCE*s of the LSC-DSSC systems. The “window−window frame” DS/UC-DSSC device with a panel area of 2 cm × 2 cm exhibited a claimed $J_{SC}$ value of 20.6 mA cm$^{-2}$ and a PCE of 9.1%, while the reported edge-mounted DSSC exhibited a short-circuit current density ($J_{SC}$) of 16.7 mA cm$^2$ with a PCE of 7.4% under AM 1.5G. The first problem is that the *PCE* of the LSC is higher than that of the edge-mounted PV, even though it absorbs only a fraction of the spectrum that the edge-mounted PV can harvest.[6,9,14] By assuming all four edges were mounted with the DSSCs, the *PCE* (and $J_{SC}$) of this LSC-

Received: November 18, 2020
Published: January 15, 2021

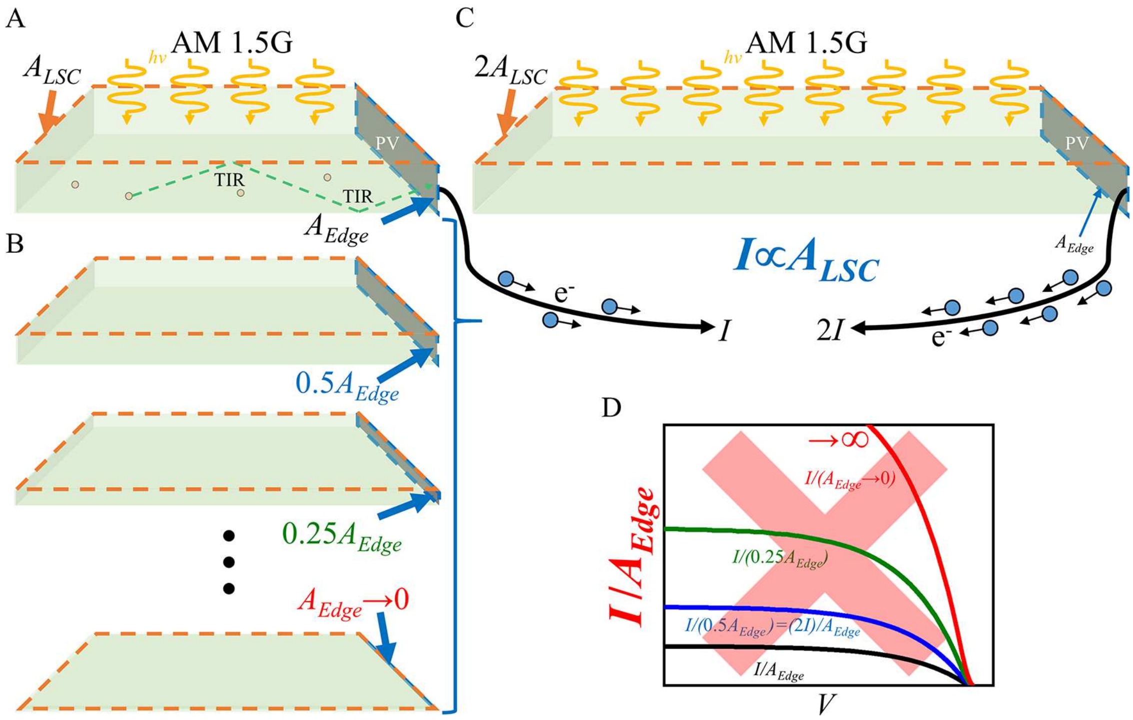


**Figure 1.** (A) Schematic of the working principle of an LSC-PV system. (B) Schematic of various LSCs with the same $A_{LSC}$ (orange dashed lines), but decreasing $A_{edge}$ (blue dashed lines). (C) Schematic of an LSC with the same $A_{edge}$, but twice the $A_{LSC}$ as the LSC shown in (A). Note: in all LSCs shown here, we assume that there is little reabsorption loss (no absorption/emission overlap) as the emitted photons waveguided to the edge-mounted PV, so that the photocurrent is ideally proportional to the waveguide front surface area ($I \propto A_{LSC}$). In most LSCs, the scaling is sublinear due to reabsorption loss. (D) Erroneously applying $A_{edge}$ in $J$−$V$ characteristics of LSCs results in significant PCE overestimation: as $A_{edge}$ decreases with constant $A_{LSC}$, the $J$ and PCE can approach infinity.

**Table 1. Photovoltaic Parameters for LSC-DSSC System with $A_{LSC}$ of 5 cm × 1 cm**

| corrected PV parameters | $J_{SC}$ (mA cm$^{-2}$) | $V_{OC}$ (V) | *FF* | *PCE* (%) | *AVT* (%) | *CRI* | ($a^*$, $b^*$) |
|---|---|---|---|---|---|---|---|
| blank | 0.144[a] | 0.71 | 0.58 | 0.06 | 92 | 100 | (0, 0) |
| DS-DSSC | 3.168[a] | 0.71 | 0.58 | 1.30 | 85.1 | 47.0 | (−18.1, 102.7) |
| DS/UC-DSSC | 3.6[a] | 0.70 | 0.58 | 1.48 | 71.3 | 41.1 | (−43.1, 90.4) |

[a]The $J_{SC}$ values are corrected by first multiplying the originally reported $J_{SC}$ values with the total $A_{edge}$ active area (1.2 cm$^2$) to obtain $I_{SC}$, then dividing $I_{SC}$ by $A_{LSC}$ (5 cm$^2$) to calculate the corrected $J_{SC}$. Parameters of aesthetic quality are also provided, where an 8% reflection loss is added to the *AVT*.

DSSC system can be estimated by applying the LSC panel area $A_{LSC}$, as shown in Table 1, resulting in a *PCE* of 1.48%.

(2) The second key data for the characterization of any photovoltaic system is the reporting of the corresponding *EQE* or internal power conversion efficiency (*IPCE*) spectrum.[10,15,16] This is necessary to calculate any spectral mismatch factors so that lamp intensities can be properly set prior to $J$−$V$ measurements or to correctly report the illumination conditions. It is also necessary for an LSC-PV system to identify any mismeasurements, such as Rayleigh scattering and direct illumination of the incident light beam,[6] and to validate the measured photocurrent density from the corresponding $J$−$V$ characteristics (just as with any other PV system).[17] The *EQE* spectra of an LSC ($EQE_{LSC}(\lambda)$) are typically position-dependent due to different reabsorption losses across the waveguide area; therefore, the correct relationship to obtain the integrated photocurrent density (Int. $J_{SC}$) from the spatially averaged $EQE_{LSC}(\lambda)$ ($EQE_{LSC}^{avg}(\lambda)$) follows:

$$\text{Int. } J_{SC} = e\int \text{AM 1.5G}(\lambda)\cdot EQE_{LSC}^{avg}(\lambda)\, d\lambda \tag{2}$$

where AM 1.5G is the solar photon flux, and $e$ is the elementary charge. Instead of providing the $EQE_{LSC}$ of the LSC-PV system, Ha et al. provided the photocurrent values at various wavelength bands by passing AM 1.5G incident light through an optical band-pass filter (Figure 3B of the original article). These results provide partial spectral information on the contribution from the LSC luminophores, but are largely incomplete and not an appropriate substitute for the $EQE_{LSC}$. For this particular LSC-DSSC system, there is little absorption−emission overlap, as shown in Figure 2, so that we assume there is negligible reabsorption loss, negligible position-dependence in $EQE_{LSC}(\lambda)$, and the $EQE_{LSC}^{avg}(\lambda)$ is approximately equal to the maximum obtainable ($EQE_{LSC}^{max}(\lambda)$). The $EQE_{LSC}(\lambda)$ is the product of loss factors, including the front surface reflection (∼4% loss), the absorption efficiency (∼100% in the wavelength ranges of 300−490 nm for the DS and 600−650 nm for the UC and ∼0 at other wavelengths), the number of emitted photons per absorbed photon (1 for the DS and 0.5 for the UC), the quantum yield (QY) (85% for the DS and 4% for the UC), waveguiding efficiency (∼75% for a waveguide with refractive index of 1.5), and $EQE_{PV}$ of the edge-mounted DSSC (∼78% in the emission range 500−600


https://dx.doi.org/10.1021/acsphotonics.0c01772
ACS Photonics 2021, 8, 678−681

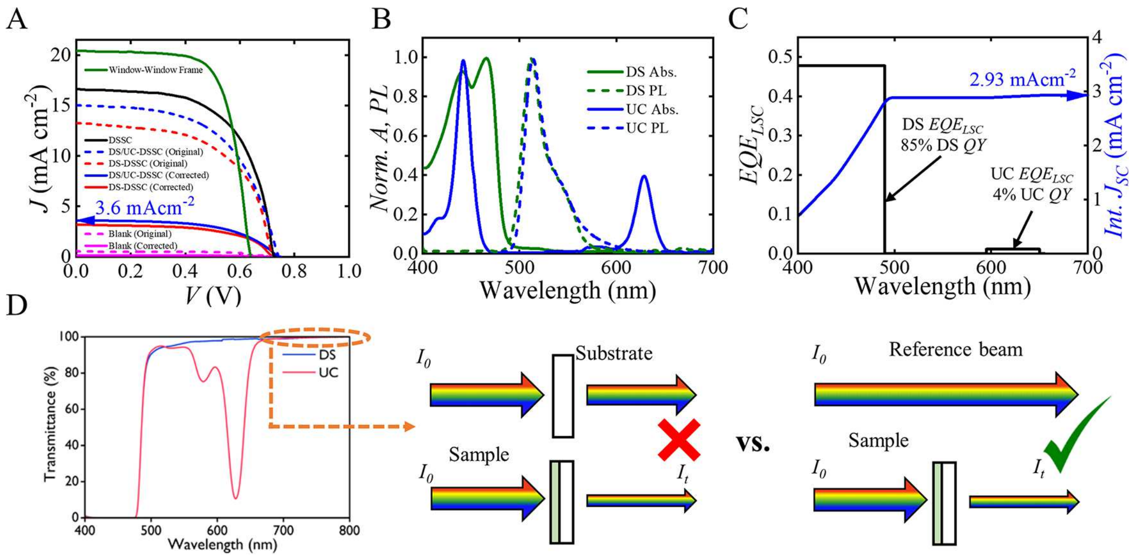


**Figure 2.** (A) $J-V$ characteristics of all LSC-DSSC systems as originally reported and corrected.[1] (B) Normalized absorption and luminescence spectra for DS-DSS and DS/UC-DSSC systems. (C) Maximum obtainable $EQE_{LSC}(\lambda)$ profile with DS $QY$ of 85% and UC $QY$ of 4% and the integrated $J_{SC}$ from the $EQE_{LSC}$ (blue right triangle), which more closely matches the corrected $J-V$ in (A). (D) Provided transmission spectrum of DS and UC LSC (left)[1] and schematic showing the comparison of incorrect/correct ways to setup the transmittance measurement for transparent PV devices (right).[7] Note: no reference sample should be utilized in double-beam spectrometers, and the dashed circle pinpoints the transmission approaching 100% in the wavelength range of 700–800 nm, indicating the presence of a reference sample.

nm). We use these values to plot the idealized $EQE_{LSC}^{max}(\lambda)$ profile of the DS/UC-DSSC system, as shown in Figure 2, which is 48% (300–490 nm) for the DS process and 1.12% (600–650 nm) for the UC process. Then the $EQE_{LSC}^{avg}(\lambda)$ profile results in an integrated photocurrent density for each process of 2.88 mA cm$^{-2}$ (DS only) and 0.045 mA cm$^{-2}$ (UC only) and a maximum total integrated photocurrent density of 2.93 mA cm$^{-2}$. This value is nearly an order of magnitude lower than the reported photocurrent density of 20.6 mA cm$^{-2}$, but it is more consistent with the maximum $J_{SC}$ that we estimate of 3.6 mA cm$^{-2}$ (provided in Table 1 and shown in Figure 2). We note that *EQE* measurements are often performed with white light bias, and this would be particularly important in this case, as the TTA process would likely be highly light intensity-dependent.

(3) To quantify the aesthetic quality of the LSC-DSSC system, Ha et al. provided the transmittance spectra of both the DS and DS/UC LSC-DSSC systems and reported the average visible light transmittance in the range of 400–700 nm was about 90% for the dual-band LSC. However, at the wavelength outside the luminophore absorption range (700–800 nm, as shown in Figure 2), the transmittance spectra approach 100%. This indicates that a reference sample (most likely a blank waveguide) was placed in the reference path of the spectrometer, which can result in an overestimation of 8–16% in average transmittance by neglecting reflection losses at the air/waveguide interfaces.[7] Correctly reporting the average visible transmittance (*AVT*) is often more important than the PCE. Color rendering index (*CRI*) and CIELAB coordinates ($a^*$, $b^*$) are also key figures of merit that are missing.[6,7] For reference, we calculate the *AVT*, *CRI* and ($a^*$, $b^*$) values (Table 1) by applying AM 1.5G as the standard illuminant and accounting for the estimated reflection loss (~8%) from a single panel to the transmission spectra.

In summary, we write this Comment to express our concern over the validity of the LSC systems reported by Ha et al.[1] We conclude that the LSC-DSSC photovoltaic performance in Ha et al. is significantly overestimated by nearly an order of magnitude. These results should not be used to benchmark other developments in the field. Based on the theoretical limits,[9] such performance could ultimately be achieved with greater material optimization, greater spectral harvesting, and improvements in quantum yields, and we encourage the community to continue striving for these performance levels. We also encourage the community to adopt standard protocols in LSC characterization[6] that parallel standard reporting requirements for all PV systems. We believe this will help advance LSC research toward a sustainable and reproducible path.

## ■ AUTHOR INFORMATION


### Corresponding Author

**Richard R. Lunt** – *Department of Chemical Engineering and Materials Science and Department of Physics and Astronomy, Michigan State University, East Lansing, Michigan 48824, United States;* orcid.org/0000-0003-4248-6312; Email: rlunt@msu.edu

### Author

**Chenchen Yang** – *Department of Chemical Engineering and Materials Science, Michigan State University, East Lansing, Michigan 48824, United States*

Complete contact information is available at: https://pubs.acs.org/10.1021/acsphotonics.0c01772


### Notes

The authors declare the following competing financial interest(s): R.R.L. is a co-founder, director, and a part owner of Ubiquitous Energy, Inc., a company working to commercialize transparent photovoltaic technologies. All other authors declare no competing financial interest.

## ■ ACKNOWLEDGMENTS

The authors gratefully acknowledge support from the National Science Foundation under Grant CBET-1702591, the James Dyson Foundation Fellowship.

## ■ REFERENCES

(1) Ha, S.-J.; Kang, J.-H.; Choi, D. H.; Nam, S. K.; Reichmanis, E.; Moon, J. H. Upconversion-Assisted Dual-Band Luminescent Solar Concentrator Coupled for High Power Conversion Efficiency Photovoltaic Systems. *ACS Photonics* **2018**, *5* (9), 3621−3627.

(2) Moor, K.; Kim, J.-H.; Snow, S.; Kim, J.-H. [C70] Fullerene-Sensitized Triplet-Triplet Annihilation Upconversion. *Chem. Commun.* **2013**, *49* (92), 10829−10831.

(3) Singh-Rachford, T. N.; Castellano, F. N. Photon Upconversion Based on Sensitized Triplet-Triplet Annihilation. *Coord. Chem. Rev.* **2010**, *254* (21), 2560−2573.

(4) Ye, C.; Gray, V.; Mårtensson, J.; Börjesson, K. Annihilation Versus Excimer Formation by the Triplet Pair in Triplet-Triplet Annihilation Photon Upconversion. *J. Am. Chem. Soc.* **2019**, *141* (24), 9578−9584.

(5) Jiang, X.; Guo, X.; Peng, J.; Zhao, D.; Ma, Y. Triplet-Triplet Annihilation Photon Upconversion in Polymer Thin Film: Sensitizer Design. *ACS Appl. Mater. Interfaces* **2016**, *8* (18), 11441−11449.

(6) Yang, C.; Liu, D.; Lunt, R. R. How to Accurately Report Transparent Luminescent Solar Concentrators. *Joule* **2019**, *3* (12), 2871−2876.

(7) Yang, C.; Liu, D.; Bates, M.; Barr, M. C.; Lunt, R. R. How to Accurately Report Transparent Solar Cells. *Joule* **2019**, *3* (8), 1803−1809.

(8) Snaith, H. J. How Should You Measure Your Excitonic Solar Cells? *Energy Environ. Sci.* **2012**, *5* (4), 6513−6520.

(9) Yang, C.; Lunt, R. R. Limits of Visibly Transparent Luminescent Solar Concentrators. *Adv. Opt. Mater.* **2017**, *5* (8), 1600851.

(10) Currie, M. J.; Mapel, J. K.; Heidel, T. D.; Goffri, S.; Baldo, M. A. High-Efficiency Organic Solar Concentrators for Photovoltaics. *Science (Washington, DC, U. S.)* **2008**, *321* (5886), 226−228.

(11) Shockley, W.; Queisser, H. J. Detailed Balance Limit of Efficiency of P-n Junction Solar Cells. *J. Appl. Phys.* **1961**, *32* (3), 510−519.

(12) Bronstein, N. D.; Yao, Y.; Xu, L.; O'Brien, E.; Powers, A. S.; Ferry, V. E.; Alivisatos, A. P.; Nuzzo, R. G. Quantum Dot Luminescent Concentrator Cavity Exhibiting 30-Fold Concentration. *ACS Photonics* **2015**, *2* (11), 1576−1583.

(13) Rafiee, M.; Chandra, S.; Ahmed, H.; McCormack, S. J. An Overview of Various Configurations of Luminescent Solar Concentrators for Photovoltaic Applications. *Opt. Mater. (Amsterdam, Neth.)* **2019**, *91*, 212−227.

(14) Henry, C. H. Limiting Efficiencies of Ideal Single and Multiple Energy Gap Terrestrial Solar Cells. *J. Appl. Phys.* **1980**, *51* (8), 4494−4500.

(15) Bergren, M. R.; Makarov, N. S.; Ramasamy, K.; Jackson, A.; Guglielmetti, R.; McDaniel, H. High-Performance CuInS2 Quantum Dot Laminated Glass Luminescent Solar Concentrators for Windows. *ACS Energy Lett.* **2018**, *3* (3), 520−525.

(16) Slooff, L. H.; Bende, E. E.; Burgers, A. R.; Budel, T.; Pravettoni, M.; Kenny, R. P.; Dunlop, E. D.; Büchtemann, A. A Luminescent Solar Concentrator with 7.1% Power Conversion Efficiency. *Phys. Status Solidi RRL* **2008**, *2* (6), 257−259.

(17) Zimmermann, E.; Ehrenreich, P.; Pfadler, T.; Dorman, J. A.; Weickert, J.; Schmidt-Mende, L. Erroneous Efficiency Reports Harm Organic Solar Cell Research. *Nat. Photonics* **2014**, *8* (9), 669−672.